

SMDP: SARS-CoV-2 Mutation Distribution Profiler for rapid estimation of mutational histories of unusual lineages

Authors: Erin E. Gill¹, Sheri Harari², Aijing Feng³, Fiona S.L. Brinkman¹, Sarah Otto^{4*}

Affiliations:

¹ Department of Molecular Biology and Biochemistry, Simon Fraser University, Burnaby, BC, Canada

² Fred Hutchinson Cancer Research Center, Howard Hughes Medical Institute, Seattle, WA, USA

³ Bond Life Sciences Center, University of Missouri, Columbia, MO, USA

⁴ Department of Zoology & Biodiversity Research Centre, University of British Columbia, Vancouver, BC, Canada

* Corresponding author: otto@zoology.ubc.ca

Keywords: COVID-19, evolution, zoonosis, chronic infection, molnupiravir, mutator lineage, saltation

Abstract

SARS-CoV-2 usually evolves at a relatively constant rate over time. Occasionally, however, lineages arise with higher-than-expected numbers of mutations given the date of sampling. Such lineages can arise for a variety of reasons, including selection pressures imposed by evolution during a chronic infection or exposure to mutation-inducing drugs like molnupiravir. We have developed an open-source web-based application (SMDP: SARS-CoV-2 Mutation Distribution Profiler; https://eringill.shinyapps.io/covid_mutation_distributions/) that compares a list of user-submitted lineage-defining mutations with established mutation distributions including those observed during (1) the first nine months of the pandemic, (2) during the global transmission of Omicron, (3) during the chronic infection of immunocompromised patients, and (4) during zoonotic spillover from humans to deer. The application calculates the most likely distribution for the user's mutation list and displays log likelihoods for all distributions. In addition, the transition:transversion ratio of the user's list is calculated to determine whether there is evidence of exposure to a mutation-inducing drug such as molnupiravir and indicates whether the list contains mutations in the proofreading domain of nsp14 which could lead to a higher-than-expected mutation rate in the lineage. This tool will be useful for public health and researchers seeking to rapidly infer evolutionary histories of SARS-CoV-2 variants, which can aid risk assessment and public health responses.

Background

SARS-CoV-2 exhibits a strong clock-like pattern of evolution, with mutational changes at a rate proportional to time, but this pattern is punctuated by “saltational” changes, where lineages suddenly appear with a higher number of mutations than expected given their divergence time from other lineages (Neher, 2022). Such lineages also show unusual distributions of mutations across the genome, often concentrating in spike, and they typically root deep in the SARS-CoV-2 tree, suggesting long periods of time out of circulation. These patterns have been observed in major variants of concern (VoC), such as Alpha, Beta, Gamma, and Delta (Neher, 2022; Otto et al., 2021). and saltational lineages continue to arise (e.g., BA.2.86*, <https://github.com/sars-cov-2-variants/lineage-proposals/issues/606>, and more recent lineages such as <https://github.com/sars-cov-2-variants/lineage-proposals/issues/1584>).

Some of these unusual lineages are thought to reflect long passage times within individuals who have weakened immune systems, sharing many of the same signatures seen in chronic infections (Harari et al., 2022). Cele et al. (2022), for example, documented evolutionary changes within a single individual over the course of 190 days that paralleled many of the mutational changes seen in VoC, resulting in heightened immune evasiveness.

When unusual lineages arise, however, it is challenging to infer the evolutionary history leading to the observed genomic changes. Other processes, including passage through animals (Bashor et al., 2021; Kotwa et al., 2023; Naderi et al., 2023), mutator lineages with error-prone polymerases (Takada et al., 2023), and exposure to mutagens such as molnupiravir (Gruber et al., 2024), may also leave unusual genomic signatures.

We developed a shiny application (https://eringill.shinyapps.io/covid_mutation_distributions/) to quantify the strength of the genomic signal in an unusual lineage for different past evolutionary environments. The application requires the user to provide the set of unique mutations leading to the lineage of interest, not including mutations that arose prior to its most recent common ancestor with other lineages. A sufficient number of mutations is needed to disentangle different genomic signatures, so we recommend the application should be used for lineages with at least 10 and preferably ≥ 20 identifying mutations (see *Power analysis*).

At present, the application compares the similarity of a user-provided list of nucleotide mutations to random draws from the following four distributions:

- A list of mutations observed during the first nine months of the pandemic, prior to the spread of VoC (Harari et al., 2022). (**global pre-VoC distribution**)
- A list of mutations observed during global transmission of Omicron (submission dates up to 25 May 2022), excluding lineage-defining mutations (Harari et al., 2022). (**global Omicron distribution**)
- A list of mutations compiled from 32 chronic infections of immunocompromised individuals (27 individuals from Harari et al., 2022, with 5 additional individuals from Harari et al. 2024) (**chronic distribution**)
- A list of mutations inferred from 109 separate zoonotic spillovers from humans to white-tailed deer (Feng et al., 2023). (**deer distribution**)

The application reports the likelihood of observing the mutation set from each of these four empirically-derived distributions, highlighting which distribution is most likely to explain the observed data and how much more likely that distribution is relative to the next most likely distribution. For these empirically-derived distributions, we consider a distribution that fits the user's mutation set >20 times better than the next best distribution to provide evidence of similarity to that distribution (see *Power analysis*).

Importantly, the application compares only a limited number of empirically-derived distributions from which a given mutation set may be drawn. Results obtained from this application thus describe the similarity only to the given distributions and do not prove that the history of the unusual lineage reflects the most likely distribution, given that other distributions – not examined – may be plausible (see *Discussion*).

While many other animals are susceptible to SARS-CoV-2, there is a very high incidence in white-tailed deer, with active infections observed in 21% of the animals tested in New York State (Feng et al., 2023). A high incidence increases the risk of a reverse spillover, from animals back to humans, as was inferred for three cases in humans (Feng et al., 2023). As more datasets compiling substantial numbers of mutations within other animal species become available, these can be added for further comparisons.

In addition, the application indicates whether the mutation set contains signals consistent with:

- Past molnupiravir use: The transition-to-transversion ratio of mutations is calculated in the focal lineage. For comparison, a background ratio of ~2:1 is typical for SARS-CoV-2, while case-control cohort studies find a higher ratio of ~14:1 under molnupiravir treatment (Gruber et al., 2024). A high ratio thus suggests past exposure to molnupiravir or a similar factor inducing transition mutations.
- Mutator lineages: Mutator alleles may contribute to the unusual features of a lineage by increasing the rate and type of mutation. Known mutators have been observed in nsp14 within the ExoN proofreading domain of SARS-CoV-2. P203L in nsp14 was shown to have an elevated substitution rate in phylogenetic analyses and was confirmed to double the mutation rate when passaged through hamsters (Takada et al., 2023). Sites F60S and C39F in nsp14 were associated with a 22-fold and 6-fold higher substitution rate in phylogenetic analyses (Mack et al., 2023). We considered mutations at sites 39, 60, and 203 in nsp14 to be known mutators and mutations in sites 90, 92, 191, 268, and 273, which fall within the ExoN proofreading domain of nsp14, to be potential mutators (Mack et al., 2023; Moeller et al., 2022).

Methods

Distribution of mutations observed globally and in chronic patients: The data from Table S4 of Harari et al. (2022), as illustrated in their Figures 1 and S1, were filtered to include mutation counts reported as "Chronic infection" to obtain the chronic distribution, "3 Global sequences (12/2019-08/2020)" to obtain the global distribution early in the pandemic (prior to VoC emergence), and "6 Omicron after emergence" to obtain the global distribution late in the

pandemic (Omicron era). Mutations in an additional five chronic infections were reported by Harari et al. (2024) and added to the “Chronic infection” set (a total of 32 patients). Mutations were placed in bins consisting of (a) 500 nucleotides, (b) 1000 nucleotides, (c) genes, or (d) genes augmented by splitting spike into pre-RBD, RBD, and post-RBD (receptor binding domain). The latter distribution is given in Table 1.

Distribution of mutations observed in white-tailed deer: Aijing Feng and Xiu-Feng Wan (pers. comm.) provided the amino acid identities of mutations that arose in or were associated with white-tailed deer (Feng et al., 2023). Feng et al. inferred the substitutions that had occurred within deer by comparing to the potential human precursor. The distribution of mutations by gene is given in Table 1 and shows a disproportionately high number of mutations in nsp3 (Figure 1).

Likelihood calculations: The [application](#) accepts a comma-separated list of nucleotide positions in the SARS-CoV-2 genome where lineage-defining mutations occur for a clade of interest. The application determines the likelihood of observing the mutation set as a random draw from each distribution (global pre-VoC, global Omicron, chronic infections, white-tailed deer). The \log_e likelihood of observing the mutation set from each distribution is displayed, as is the relative likelihood of seeing the data from the best fitting distribution relative to the next best fitting.

\log_e likelihoods were calculated from the multinomial probability of drawing the mutation set from an empirically-based distribution. Given a user-defined bin size (500 nucleotides, 1000 nucleotides, genes, or genes augmented by spike), the probability of observing k_i mutations in the mutation set when there were n_i in the empirical distribution was calculated for each bin i .

Taking the natural log and summing over bins yields the overall \log_e likelihood:

$$\ln L = \sum_i k_i \ln\left(\frac{n_i+1}{\sum_j (n_j+1)}\right)$$

The addition of one to the empirically-derived distribution counts ($n_i + 1$) ensures that no bins lack data and is expected to have a conservative effect on the results (making all distributions slightly more similar).

Power analysis: We assessed the statistical properties of the relative likelihoods of observing the mutation set from the different empirically-derived distributions, estimating the false positive rate and the false negative rate (power). To estimate the false positive rate, we determined how often randomly drawn mutation sets from the global pre-VoC distribution would suggest a misleadingly high probability of being drawn from the chronic or deer distributions (Figure 2A). Using a threshold of 20-fold for rejecting the null hypothesis of the global distribution in favor of another distribution, <1% of 10,000 randomly generated mutation sets yielded a false positive result (e.g., favoring the chronic distribution in 0.46%, 0.55%, 0.31%, 0.11%, 0.01% of replicates for mutation sets of size 5, 10, 20, 40, and 80, respectively). A threshold of 10-fold also yielded reasonable false positive rates (<2%) for the cases tested.

To estimate the false negative rate (power), we determined how often randomly drawn mutation sets from the chronic distribution would yield a strong enough signal to reject the global pre-VoC distribution (Figure 2B). Using a threshold of 20-fold for rejecting the null hypothesis of the global distribution in favor of the chronic distribution, mutation sets with at least 10 mutations led to a rejection of the null hypothesis in the majority of replicates (>50%), with power rising to >80% with at least 20 mutations in the set.

Application Example

As an example, we consider B.A.2.86, a highly divergent variant that was identified as an unusual lineage on 13 August 2023 by Hynn Spylor (<https://github.com/sars-cov-2-variants/lineage-proposals/issues/606>). The lineage bears 41 mutational differences from its most recent common ancestor with BA.2 (diverging ~2 years ago) and dispersed rapidly (found in 8 countries by the end of August).

The 41 lineage-defining mutations were listed by Ryan Harris (<https://github.com/cov-lineages/pango-designation/issues/2183>) as:

```
{C897A,G3431T,A7842G,C8293T,G8393A,G11042T,C12789T,T13339C,T15756A,A18492G,ins  
21608,C21711T,G21941T,T22032C,C22208T,A22034G,C22295A,C22353A,A22556G,G22770A  
,G22895C,T22896A,G22898A,A22910G,C22916T,del23009,G23012A,C23013A,T23018C,T230  
19C,C23271T,C23423T,A23604G,C24378T,C24990T,C25207T,A26529C,A26610G,C26681T,C2  
6833T,C28958A}
```

where we have excluded A12160G, considered in the thread to be a rooting problem. The results shown by the [application](#)'s analysis of the above mutation set are illustrated in Figure 1. The results indicate that this unusually divergent BA.2.86 variant most likely evolved as a result of a chronic infection, among the distributions compared here.

Discussion

Understanding the recent history of a virus, especially a genetically unusual virus, can help us to reduce future risks: identifying and clearing chronic infections globally, reducing the risks of treatments that are mutagens, and minimizing risks of spillover events. This application attempts to rapidly aid the interpretation of newly appearing, unusual SARS-CoV-2 lineages by quantifying similarity to signals left by past selection and mutation pressures.

There are several caveats to be kept in mind when interpreting the results. Most importantly, interpreting the relative probability of explaining the observed mutation set is limited to the set of distributions compared. Just because the lineage-defining mutations of an unusual lineage is more consistent with the distribution of mutations observed in chronically infected individuals than the global distribution does not prove that the lineage passaged through chronically infected individuals, given that not all possible distributions are included.

In particular, we lack distributions of evolutionary changes from global transmission events in the recent past (the Omicron-era sequences analysed by Harari et al., included submission dates only up to 25 May 2022), which might provide a more relevant comparison for the unusual lineages appearing today. Because the application requires sufficient depth of information for mutations throughout the genome, the many other animal species that could be reservoirs (Chakraborty et al., 2024) are also not included.

There are additional pieces of information that could be used to infer the evolutionary history of SARS-CoV-2 lineages. We have not used information about the rate of mutations per unit time, whether the mutations are silent or coding, or the specific nature of the amino acid changes induced.

If users have unaligned SARS-CoV-2 genome sequences that they would like to use as input for this tool, they must first place them into a phylogeny to detect lineage-defining mutations. To get started, helpful tools can be found on the UCSC SARS-CoV-2 Genome Browser (<https://genome.ucsc.edu/goldenPath/help/covidBrowserIntro.html#data>). Users can also visualize and export mutations relative to the founder of the clade that a sequence belongs to using NextClade (<https://clades.nextstrain.org/>).

Nevertheless, we intend the application to be used as a quick means of categorizing the unusual features in a set of mutations that define a SARS-CoV-2 lineage. Additional mutation distributions could be added in the future.

Data availability

The *Mathematica* code used to process the data and generate Figure 2 and the Python code to produce the shiny application and Figure 1 are available on Zenodo (DOI: [10.5281/zenodo.12735051](https://doi.org/10.5281/zenodo.12735051)).

Acknowledgements

We thank all researchers for their investigations of mutation distributions, which enabled development of this SMDP application. SMDP was developed by members of the Computational Analysis, Modelling and Evolutionary Outcomes (CAMEO <https://covarnet.ca/computational-analysis-modelling-and-evolutionary-outcomes-cameo/>) pillar of Canada's Coronavirus Variants Rapid Response Network (CoVaRR-Net <https://covarnet.ca/>), with further input by other members of this CAMEO group and the Brinkman Lab. CAMEO is supported by Genome Canada, Innovation, Science and Economic Development Canada (ISED) and the Canadian Institutes of Health Research (CIHR) (grant #ARR-175622). This project was supported by funding from a CoVaRR-Net Rapid Response Research Grant. FSLB is an SFU Distinguished Professor.

Table 1: Distributions compared. For each genetic region, the start and end positions were based on NCBI Reference Sequence [NC_045512.2](#), with the receptor binding domain of spike spanning amino acid positions 331-524 as given by (Tai et al., 2020). The distributions of mutation counts are from transmissions within the global data set, either early in the pandemic or late in the Omicron era (Harari et al., 2022), chronic infections (Harari et al., 2022), or white-tailed deer (Feng et al., 2023).

Genomic segment	Start	End*	Global [early]	Global [late]	Chronic	Deer
nsp1	266	805	23	40	9	19
nsp2	806	2719	59	152	14	58
nsp3	2720	8554	148	439	47	204
nsp4	8555	10054	34	87	11	56
proteinase	10055	10972	27	75	4	20
nsp6	10973	11842	26	66	7	34
nsp7	11843	12091	4	14	2	9
nsp8	12092	12685	12	30	4	22
nsp9	12686	13024	11	26	1	4
nsp10	13025	13441	6	20	0	6
polymerase	13442	16236	68	143	19	34
helicase	16237	18039	35	104	12	21
nsp14 (exonuclease)	18040	19620	35	99	11	30
endoRNase	19621	20658	29	36	6	49
methyltransferase	20659	21552	19	48	4	18
S (NTD)	21563	22552	43	117	42	63
S (RBD)	22553	23134	13	148	44	7
S (post RBD)	23135	25384	52	156	20	57
ORF3a	25393	26220	66	106	6	46
E	26245	26472	6	16	13	2
M	26523	27191	18	82	8	10
ORF6	27202	27387	9	23	3	11
ORF7a	27394	27759	15	43	8	30
ORF7b	27756	27887	9	22	2	7
ORF8	27894	28259	22	28	7	30
N	28274	29533	83	153	12	51
ORF10	29558	29674	6	20	0	0
Total			930	2398	316	898

* The end of the genic region is set to the nucleotide just before the next genic region, ensuring that all nucleotides from 266-29674 are counted once, regardless of the end of the coding region.

Figure 1: Usage example. The lineage-defining mutations in BA.2.86 were used to illustrate the application. The BA.2.86 lineage showed a typical ratio of transitions to transversions (Gruber et al., 2024) and did not carry changes at known mutator sites (Takada et al., 2023). The lineage-defining mutations better matched the chronic distribution than the other distributions (lnL values of -107.51 for the chronic distribution, -137.50 for the global [early] distribution, -116.96 for the global [late] distribution, -144.42 from the deer distribution), being ~13000 times more likely to be drawn from the chronic distribution than the the late global distribution from the Omicron era, the next best matching distribution.

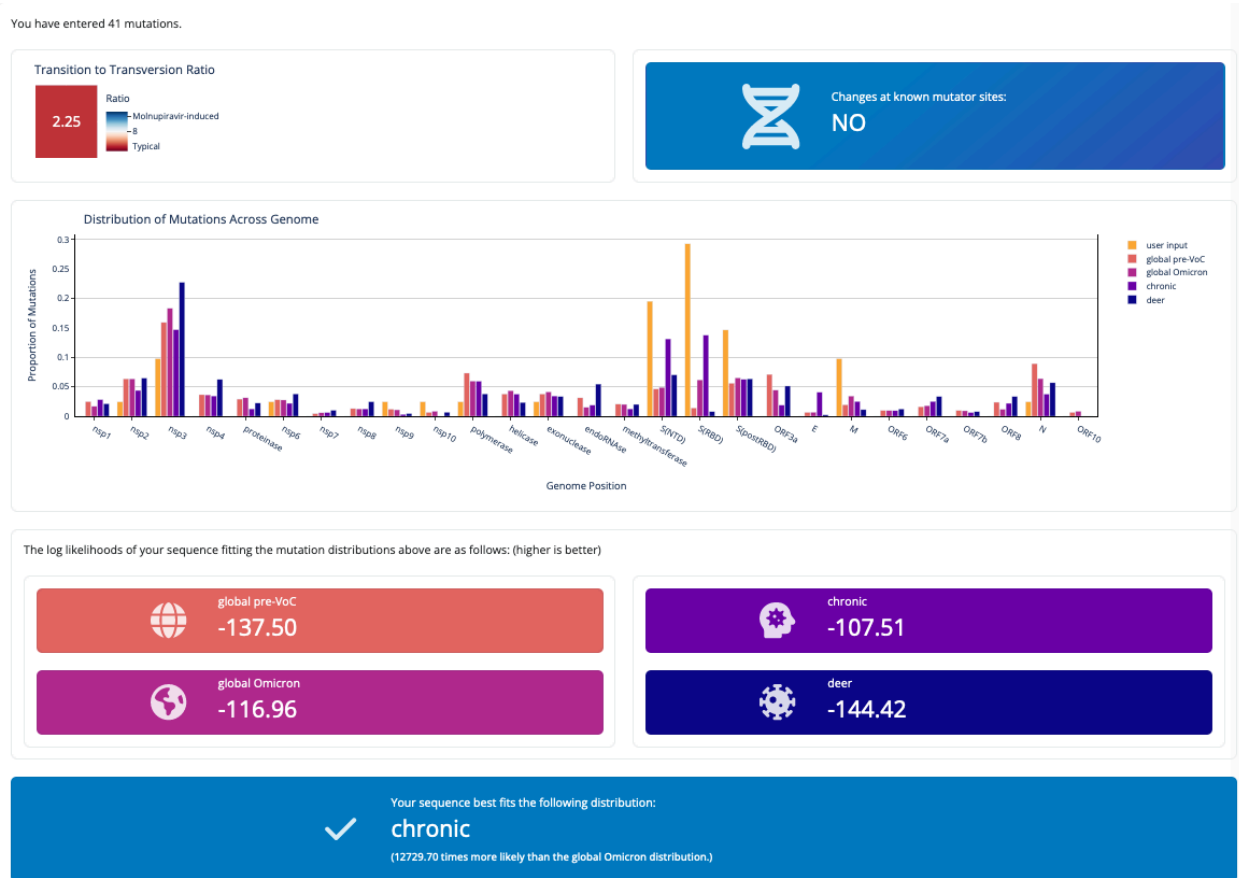
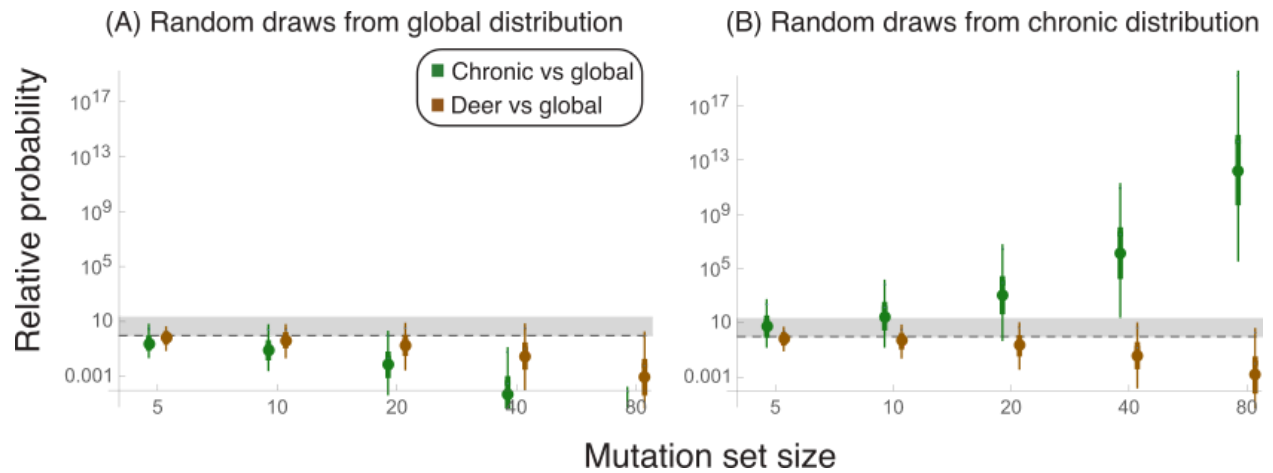


Figure 2: Power analysis. Mutation sets of different sizes (x axis) were drawn at random from either (A) the distribution of global mutations (pre-VoC) or (B) the distribution of chronic mutations (Harari et al., 2022). The null hypothesis that the set is drawn from the global distribution is then tested against the alternative hypothesis that it comes from the chronic (green) or deer (brown) distribution. Relative probabilities (y axis) greater than 20 (above grey shaded region) are rarely seen when the null hypothesis is true (panel A), but become increasingly likely as the size of the mutation set increases when the null hypothesis is false (panel B). Each distribution is obtained from 10,000 replicate mutation sets, with the median (circle), 25-75% quantiles (wide bar), and 2.5-97.5% quantiles (thin bar) illustrated.



References

- Bashor, L., Gagne, R. B., Bosco-Lauth, A. M., Bowen, R. A., Stenglein, M., & VandeWoude, S. (2021). SARS-CoV-2 evolution in animals suggests mechanisms for rapid variant selection. *Proceedings of the National Academy of Sciences of the United States of America*, *118*(44). <https://doi.org/10.1073/pnas.2105253118>
- Cele, S., Karim, F., Lustig, G., San, J. E., Hermanus, T., Tegally, H., Snyman, J., Moyo-Gwete, T., Wilkinson, E., Bernstein, M., Khan, K., Hwa, S.-H., Tilles, S. W., Singh, L., Giandhari, J., Mthabela, N., Mazibuko, M., Ganga, Y., Gosnell, B. I., ... Sigal, A. (2022). SARS-CoV-2 prolonged infection during advanced HIV disease evolves extensive immune escape. *Cell Host & Microbe*, *30*(2), 154–162.e5.
- Chakraborty, C., Bhattacharya, M., Islam, M. A., Zayed, H., Ohimain, E. I., Lee, S.-S., Bhattacharya, P., & Dhama, K. (2024). Reverse Zoonotic Transmission of SARS-CoV-2 and Monkeypox Virus: A Comprehensive Review. *Journal of Microbiology* . <https://doi.org/10.1007/s12275-024-00138-9>
- Feng, A., Bevins, S., Chandler, J., DeLiberto, T. J., Ghai, R., Lantz, K., Lenocho, J., Retchless, A., Shriner, S., Tang, C. Y., Tong, S. S., Torchetti, M., Uehara, A., & Wan, X.-F. (2023). Transmission of SARS-CoV-2 in free-ranging white-tailed deer in the United States. *Nature Communications*, *14*(1), 4078.
- Gruber, C. E. M., Tucci, F. G., Giombini, E., Mazzotta, V., Spezia, P. G., Rueca, M., Mastrosera, I., Fabeni, L., Berno, G., Butera, O., Rosati, S., Specchiarello, E., Carletti, F., Focosi, D., Nicastrì, E., Girardi, E., Antinori, A., & Maggi, F. (2024). Molnupiravir increases SARS-CoV-2 genome diversity and complexity: A case-control cohort study. *Journal of Medical Virology*, *96*(5), e29642.
- Harari, S., Miller, D., Fleishon, S., Burstein, D., & Stern, A. (2024). Using big sequencing data to identify chronic SARS-Coronavirus-2 infections. *Nature Communications*, *15*(1), 648.
- Harari, S., Tahor, M., Rutsinsky, N., Meijer, S., Miller, D., Henig, O., Halutz, O., Levytskyi, K., Ben-Ami, R., Adler, A., Paran, Y., & Stern, A. (2022). Drivers of adaptive evolution during chronic SARS-CoV-2 infections. *Nature Medicine*, *28*(7), 1501–1508.
- Kotwa, J. D., Lobb, B., Massé, A., Gagnier, M., Aftanas, P., Banerjee, A., Banete, A., Blais-Savoie, J., Bowman, J., Buchanan, T., Chee, H.-Y., Kruczkiewicz, P., Nirmalarajah, K., Soos, C., Vernygora, O., Yip, L., Robbin Lindsay, L., McGeer, A. J., Maguire, F., ... Mubareka, S. (2023). Genomic and transcriptomic characterization of delta SARS-CoV-2 infection in free-ranging white-tailed deer (*Odocoileus virginianus*). *iScience*, *26*(11). <https://doi.org/10.1016/j.isci.2023.108319>
- Mack, A. H., Menzies, G., Southgate, A., Jones, D. D., & Connor, T. R. (2023). A Proofreading Mutation with an Allosteric Effect Allows a Cluster of SARS-CoV-2 Viruses to Rapidly Evolve. *Molecular Biology and Evolution*, *40*(10). <https://doi.org/10.1093/molbev/msad209>
- Moeller, N. H., Shi, K., Demir, Ö., Belica, C., Banerjee, S., Yin, L., Durfee, C., Amaro, R. E., & Aihara, H. (2022). Structure and dynamics of SARS-CoV-2 proofreading exoribonuclease ExoN. *Proceedings of the National Academy of Sciences of the United States of America*, *119*(9). <https://doi.org/10.1073/pnas.2106379119>
- Naderi, S., Chen, P. E., Murall, C. L., Poujol, R., Kraemer, S., Pickering, B. S., Sagan, S. M., & Shapiro, B. J. (2023). Zooanthroponotic transmission of SARS-CoV-2 and host-specific

viral mutations revealed by genome-wide phylogenetic analysis. *eLife*, 12.
<https://doi.org/10.7554/eLife.83685>

- Neher, R. A. (2022). Contributions of adaptation and purifying selection to SARS-CoV-2 evolution. *Virus Evolution*, 8(2), veac113.
- Otto, S. P., Day, T., Arino, J., Colijn, C., Dushoff, J., Li, M., Mechai, S., Van Domselaar, G., Wu, J., Earn, D. J. D., & Ogden, N. H. (2021). The origins and potential future of SARS-CoV-2 variants of concern in the evolving COVID-19 pandemic. *Current Biology: CB*, 31(14), R918–R929.
- Tai, W., He, L., Zhang, X., Pu, J., Voronin, D., Jiang, S., Zhou, Y., & Du, L. (2020). Characterization of the receptor-binding domain (RBD) of 2019 novel coronavirus: implication for development of RBD protein as a viral attachment inhibitor and vaccine. *Cellular & Molecular Immunology*, 17(6), 613–620.
- Takada, K., Ueda, M. T., Shichinohe, S., Kida, Y., Ono, C., Matsuura, Y., Watanabe, T., & Nakagawa, S. (2023). Genomic diversity of SARS-CoV-2 can be accelerated by mutations in the nsp14 gene. *iScience*, 26(3), 106210.

Table S1: Known and potential mutator sites. Known sites have been confirmed experimentally, and the specific amino acid / nucleotide changes leading to mutator phenotypes are shown (“Confirmed” in “Site Type” column). Potential sites lie within the ExoN proofreading domain of Nsp14, as shown in Mack et al. (2023) (“Potential” in “Site Type” column). The wild type amino acids and positions within the mature Nsp14 protein, as well as the genomic locations of the encoding nucleotides, are shown for these sites, but changes that would lead to mutator phenotypes have not been confirmed.

Gene	Amino Acid Change	Nucleotide Change	Site Type	Reference
nsp14	C39F	G18155T	Confirmed	(Mack et al. 2023)
nsp14	F60S	T18218C	Confirmed	(Takada et al. 2023)
nsp14	P203L	C18647T	Confirmed	(Mack et al. 2023)
nsp14	D90	18307-18309 (GAT)	Potential	(Mack et al. 2023)
nsp14	E92	18313-18315 (GAG)	Potential	(Mack et al. 2023)
nsp14	E191	18610-18612 (GAG)	Potential	(Mack et al. 2023)
nsp14	H268	18841-18843 (CAT)	Potential	(Mack et al. 2023)
nsp14	D273	18856-18858 (GAT)	Potential	(Mack et al. 2023)